



Development of an evolved gas-time-of-flight mass spectrometer for the Volatile Analysis by Pyrolysis of Regolith (VAPoR) instrument

Stephanie A. Getty^{a,*}, Inge L. ten Kate^{a,b}, Steven H. Feng^a, William B. Brinckerhoff^a, Eric H. Cardiff^a, Vincent E. Holmes^{a,c}, Todd T. King^a, Mary J. Li^a, Erik Mumm^d, Paul R. Mahaffy^a, Daniel P. Glavin^a

^a NASA Goddard Space Flight Center, 8800 Greenbelt Road, Greenbelt, MD 20771, USA

^b Goddard Earth Science and Technology Center, 5523 Research Park Drive, Suite 320, University of Maryland Baltimore County, Baltimore, MD 21228, USA

^c Bastion Technologies, 7535 Mission Drive, Lanham, MD 20706-2291, USA

^d Honeybee Robotics, 460W. 34th Street, New York, NY 10001, USA

ARTICLE INFO

Article history:

Received 9 April 2010

Received in revised form 17 June 2010

Accepted 18 June 2010

Available online 30 June 2010

Keywords:

Time-of-flight

Pyrolysis

Planetary science

Mass spectrometry

Field emission

Carbon nanotube

ABSTRACT

Low power, robust technologies are appealing for in situ planetary science throughout the Solar System. The VAPoR (Volatile Analysis by Pyrolysis of Regolith) instrument is under development toward studying soil composition, volatiles, and trapped noble gases in the polar regions of the Moon and on the surface of other airless bodies. VAPoR will ingest a soil sample and conduct analysis by pyrolysis and time-of-flight mass spectrometry (ToF-MS). Two components of the system have been characterized in parallel development: a field-tested sample heater design and a laboratory-based time-of-flight mass spectrometer that emphasizes reduced mass and power through the use of micro- and nanotechnology. The pyrolysis field unit, vacuum-coupled to a commercial residual gas analyzer, has been used in Hawaii to analyze Mauna Kea soils. Water was detected, as were key inorganic pyrolysis products, including CO₂ and SO₂, and organic volatiles, including methane, benzene, toluene, and various hydrocarbon fragments. In parallel development, a laboratory reflectron time-of-flight mass spectrometer has been designed, assembled, and tested using electron impact ionization from a carbon nanotube electron gun. Preliminary testing reveals a mass resolution of 270.

Published by Elsevier B.V.

1. Introduction

Measuring the chemical composition of solid bodies in our Solar System is key to understanding the formation and evolution of the planets and their moons. One possible instrument for in situ chemical analysis of planetary atmospheres and surface regolith is VAPoR, Volatile Analysis by Pyrolysis of Regolith [1]. As part of a landed or roving mission to the surface of a solid body, VAPoR enables compositional and isotopic measurements of volatiles released from solid surface samples on airless bodies including the Moon, asteroids, comets, and the icy moons of the Outer Planets. With the addition of a miniature turbo-pump, VAPoR could also operate in higher

pressure environments including Mars and Titan. As depicted in Fig. 1, VAPoR combines a sample carousel of 6 individually heated pyrolysis ovens with a miniaturized, low-power and low-mass time-of-flight mass spectrometer (ToF-MS). Powdered or ground soil samples collected by a rover or lander sample acquisition system and delivered to the VAPoR ovens can be heated to temperatures up to 1200 °C to liberate the volatile constituents for direct measurement by the ToF-MS. Two independent units have been built and tested to understand the performance of the different instrument components. A laboratory breadboard was developed to test and calibrate the ToF-MS, and a portable field unit consisting of a custom made high temperature pyrolysis oven, coupled to a commercial RGA mass spectrometer via a vacuum system, was built to demonstrate the feasibility of conducting vacuum pyrolysis evolved gas measurements in the field.

Calibration of the VAPoR field unit can help to identify the bulk chemistry of the soil samples, including the presence of water, hydrocarbons, noble gases, and evolved gas signatures corresponding to carbonates, sulfates, and nitrates. Evidence for aqueous alteration and the presence of water and hydrocarbons in planetary regolith will provide insight into the occurrence of astrobiology-

* Corresponding author at: NASA Goddard Space Flight Center, Materials Engineering Branch, Mailstop 541.0, Greenbelt, MD 20771, USA. Tel.: +1 301 286 9760.
E-mail addresses: stephanie.a.getty@nasa.gov (S.A. Getty),

inge.l.tenkate@nasa.gov (I.L. ten Kate), steven.h.feng@nasa.gov (S.H. Feng), william.b.brinckerhoff@nasa.gov (W.B. Brinckerhoff), eric.h.cardiff@nasa.gov (E.H. Cardiff), vincent.holmes@nasa.gov (V.E. Holmes), todd.t.king@nasa.gov (T.T. King), mary.j.li@nasa.gov (M.J. Li), mumm@honeybeerobotics.com (E. Mumm), paul.r.mahaffy@nasa.gov (P.R. Mahaffy), daniel.p.glavin@nasa.gov (D.P. Glavin).

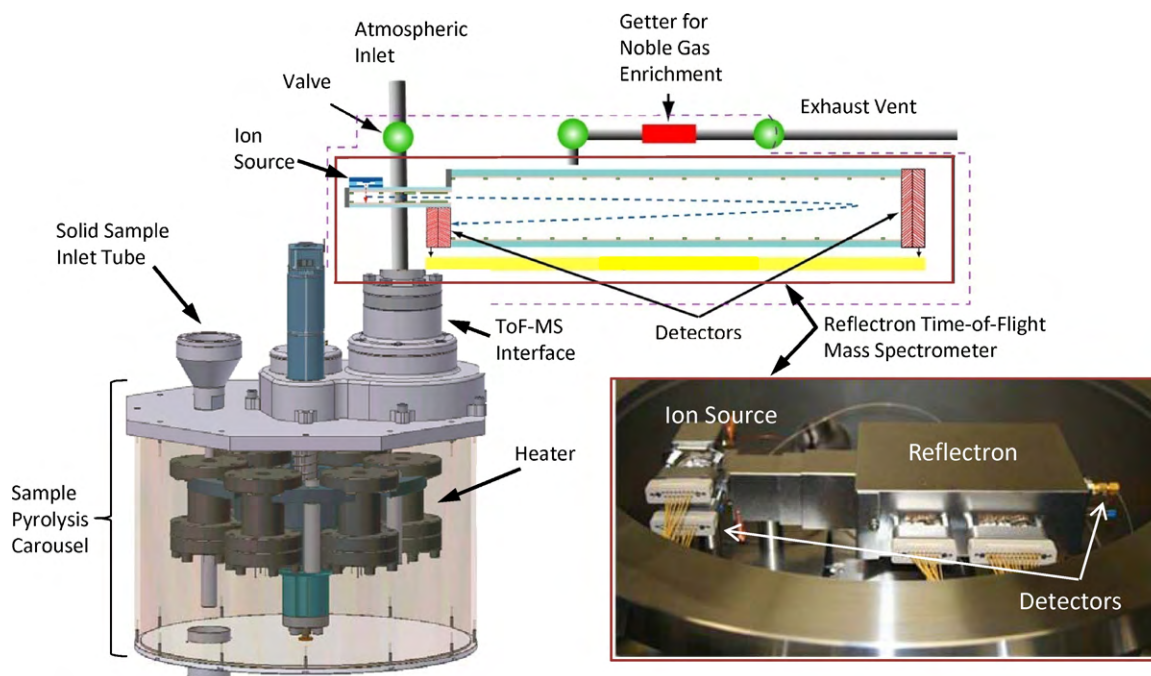


Fig. 1. The VAPoR instrument will combine a sample pyrolysis carousel containing six separate ovens with a low-power, miniaturized time-of-flight mass spectrometer for volatile analyses on the surface of planetary bodies throughout the Solar System.

relevant constituents on planetary bodies. To reach some of these remote destinations, the instrument payload will be necessarily compact and low power; therefore, one of the objectives of the VAPoR development is to reduce the power and mass required to perform these measurements. To this end, the ToF-MS component of VAPoR is designed to employ a number of technological advances to allow power and mass reduction in a high performance instrument. Micro- and nanotechnology have been used to design and build a ToF-MS prototype that has undergone preliminary testing and calibration. This instrument development will be discussed in Section 3.

VAPoR is a new descendant in a well-established family of both spaceflight mass spectrometers and evolved gas analyzers. As early as 1975, the Viking landers each carried pyrolysis-gas chromatograph-mass spectrometer (GC-MS) instruments to the surface of Mars. The Viking oven design heated soils in one of three pyrolysis ovens to a temperature of 500 °C, delivered the volatiles to a GC column for chromatographic separation, and used a quadrupole mass filter to acquire a mass spectrum. More recently, an evolved gas analyzer (EGA) was integrated with a differential scanning calorimeter (DSC) on the Phoenix lander that arrived at the Mars northern latitudes in 2008. Soil was introduced into one of the eight nickel ovens, and detection of major constituents of the evolved gases was conducted by a miniature magnetic sector mass spectrometer [2]. To continue the study of the Martian surface, the Sample Analysis at Mars (SAM) instrument suite [3] has been developed for the Mars Science Laboratory rover [4], currently scheduled for launched in 2011. The instrument suite will provide pyrolysis capability up to a temperature of 1000 °C for 74 individual sample cups located in a two-ringed carousel developed by Honeybee Robotics. Nine of these 74 cups are hermetically sealed metal wet chemistry cups, containing a derivatization fluid that will react with the soil and enhance the detection capability of organics in surface materials such as amino and carboxylic acids that would not otherwise be detected by pyrolysis GC-MS alone. Analysis of evolved species and atmospheric gases will be separated by one of 6 gas chromatography (GC) columns and can be

detected by thermal conductivity (TCD) and the quadrupole mass spectrometer (QMS). The QMS exhibits unit mass resolution over a mass range of 2–535 Da. A tunable laser spectrometer (TLS) is also included in the instrument suite to determine isotopic ratios of carbon and oxygen in atmospheric CH₄ and CO₂. Slated to land at one of several candidate sites suggesting past water activity and possible preservation of organics, the SAM instrument suite is expected to greatly enhance our understanding of the habitability of Mars.

Mass spectrometers have furthermore been deployed on orbiting spacecraft, such as the Cassini-Huygens mission, which targeted the compositions of Saturn and its hydrocarbon-rich moon Titan. The Cassini orbiter sampled ions and neutrals while orbiting Saturn [5], and the Huygens probe descended through the thick Titan atmosphere to the surface while analyzing atmospheric and volatile constituents with a gas chromatograph-quadrupole mass spectrometer [6]. Quadrupole mass spectrometers have a strong heritage for spaceflight, but recently, time-of-flight instruments have been the focus of spaceflight development as well. For example, a time-of-flight mass spectrometer was developed for the ROSINA instrument [7] of the ROSETTA mission to the surface of a comet. Coupled to a double-focusing magnetic sector MS with mass range of 12–150 Da and resolution of $m/\Delta m = 3000$, the ROSINA ToF-MS features a mass range of 1–300 Da, with mass resolution of 500 Da, and is geared to understanding the chemical and isotopic composition of a cometary atmosphere.

Upcoming missions to remote planetary surfaces will require smaller and simpler instruments than some of these predecessors. The resources available on future robotic missions to the Moon, comets and asteroids, and icy moons will likely not be able to support a complex instrument. Therefore, the development of lower mass, power, and volume evolved gas mass spectrometers for these resource-constrained missions is essential. For this reason, our development efforts focus on achieving sufficient performance to achieve the following science objectives: (1) detect and measure the presence of water and noble gases, and (2) determine the presence of aliphatic and aromatic hydro-

carbons, and small O- and N-containing organics. The VAPoR instrument in development consists of two major components: the pyrolysis ovens and the reflectron time-of-flight mass spectrometer, with a sub-development on the field emission electron gun. These components are currently the subject of parallel development efforts and therefore will be discussed in three different sections.

2. Pyrolysis mass spectrometry and evolved gas analysis

Evolved gas analysis by vacuum pyrolysis is the most efficient technique to release and analyze the widest range of volatiles from a solid sample [8]. Pyrolysis mass spectrometry and evolved gas analysis techniques have been studied since over a century [9–12] and are widely used in planetary science missions [3,8,13–16]. The technique relies on the thermal release and breakdown of volatiles and different constituents of a solid sample's mineralogy and organic composition at different temperatures. The pyrolysis temperature of each chemical compound depends on various factors, such as the tendency of the species to sublime, the binding energy of a volatile molecule to a host matrix, the energy required to break a critical bond (conversion of carbonate to CO₂, for example), and even the microstructure of a sample, i.e., the location of encapsulated phases with respect to the sample surface. Calibration is therefore a key development step toward interpreting the thermal profile of evolved gases from a variety of different mineral standards.

The VAPoR prototype pyrolysis oven, derived from the SAM pyrolysis ovens, consists of a resistively heated sample cup enclosed in radiation shielding. The sample cup is made of conical single-stranded tungsten wire conformally coated with zirconia ceramic (R. D. Mathis Co.) that can accept ~0.4 cm³ of solid sample and heat the contents to at least 1200 °C, higher than the current maximum temperature for SAM. The higher target temperature for VAPoR is required to release oxygen from silicate minerals and some noble gas species that are only released from high temperature mineral phases above 1200 °C. Seven concentric radiation shields surround the cup to mitigate heat loss to the outside. A conical housing encloses the oven and shielding to maintain a vacuum and is interfaced directly to the inlet of the mass spectrometer via a vacuum manifold. Power is supplied to the heater coil and ramped to increase regolith temperature at a controlled rate. Recent laboratory tests have demonstrated a linear ramp from ambient up to a temperature of 1200 °C, requiring a power of 144 W at maximum temperature. Future optimization of the crucible design is currently underway to reduce the current and power usage of the VAPoR oven crucible. For these experiments a commercial residual gas analyzer (RGA) from Stanford Research Systems was used to acquire mass spectra and measure volatile outgassing as a function of time/heater temperature. Similar measurements are also planned for the miniature ToF-MS when it is integrated to the VAPoR unit. Alternatively, atmospheric sample gas can bypass the pyrolysis stage by being sampled through an inlet valve for direct mass analysis.

In future instrument development, six pyrolysis heaters will be integrated into a robotic sample carousel, currently in development at Honeybee Robotics, NY, that will allow the acquisition and analysis of at least six different regolith samples during an autonomous robotic mission to a planetary surface. During a pyrolysis experiment, the heater assembly is robotically elevated in the housing to form a vacuum seal with the mass spectrometer inlet. A known volume of regolith will be introduced through a solid sample inlet tube that can be ultrasonically modulated and heated to mitigate the risk of sample clogging.

3. Time-of-flight mass spectrometer

Important features of the ToF-MS under development for VAPoR applications include sufficiently high beam current for efficient ionization, sufficiently long lifetime for autonomous in situ operation during a planetary mission, and low power operation to meet the requirements of a resource-constrained mission opportunity.

During design and fabrication of the ToF-MS components, an emphasis was placed on miniaturization, ultra-clean packaging, and low power operation. The time-of-flight mass spectrometer operates by ionizing a sample gas by electron impact, accelerating the ions to a known kinetic energy using an electric field, and allowing the ions to separate in time along a single trajectory according to their masses, as described by classical mechanics. For a known kinetic energy, KE, and flight path length, *L*, we can describe the time-of-flight, *t*, as a function of mass, *m*:

$$t = L \sqrt{\frac{m}{2KE}}$$

Heavier masses will exhibit a longer time-of-flight than lighter masses, from which a mass spectrum can be derived. The longer the flight path, *L*, the better the (temporal) separation between two adjacent masses. As a result, there is a competition between mass resolution and instrument size in the miniaturization of a ToF-MS. The use of a reflectron can compensate for this limited mass resolution. Using an electrostatic ion mirror, ion packets traveling from the ion source into the reflectron are impeded by “uphill” electric potential contours and each ion's motion is reversed (Fig. 2).

When the detector is placed at the appropriate focal plane, the use of a reflectron can double the flight path while maintaining a small instrument footprint. Extensive simulations of the performance of the ToF-MS instrument prototype have been conducted using a commercial electrostatics package, SIMION. A model has been constructed that incorporates the electron gun, ion lens assembly, reflectron, and position of the detector plane. A model based on the current geometry of the ToF-MS instrument, as shown in Fig. 3, predicts unit mass resolution at 600 Da.

In the VAPoR ToF-MS, the ion source consists of a field emission electron gun for electron impact ionization and an ion lens assembly. The electron gun is positioned such that the electron beam is perpendicular to the ion trajectories. Ions are then accelerated into a reflectron analyzer with a short voltage pulse on the extraction lens, marking *t* = 0. The detector is positioned either at the end of the reflectron (for linear mode operation) or beneath the ion source (for reflected mode operation). The detector is a commercial chevron microchannel plate device (Photonis, Inc.).

Modular ion source and reflectron components were constructed from distinct sections of dissipative substrate. This dissipative substrate (Photonis, Inc.) is sufficiently resistive to support a smoothly varying potential difference between adjacent lens traces with low current draw, while providing a sufficiently conductive surface to dissipate charge build-up that can lead to spurious and unpredictable electric fields that can adversely affect the charged particle trajectories within the instrument. Transient charging effects can lead to reduced instrument sensitivity and diminished mass resolution.

Both ion source and reflectron used parallel plate configurations to achieve electric field uniformity in the “sweet spot” of the instrument. To form the electrostatic lenses, thin film metal traces were defined using electron beam deposition in a base vacuum of 10⁻⁷ Torr. Machinable Rescor[®] ceramic was used to retain each plate, and press-fit pogo pins were then used to electrically connect each lens trace. Threaded rod hardware was used to maintain separation between the lens plates.

To produce the electric potential profiles needed for ionization and analysis, a monolithic lens architecture was used. Instead of

precision assembly of discrete electrostatic lens elements, a planar, electrically dissipative substrate was patterned with metal traces using silicon microfabrication techniques.

The ion source parallel plates are spaced by only a few millimeters; as a result, fringing fields are minimal and confined primarily to the remote edges of the ion lens assembly. The reflectron plates,

in contrast, are spaced by a distance that is comparable to the plate dimensions. Therefore, discrete metal sidewalls were installed to mitigate fringing fields bleeding into the bulk of the analyzer. A consequence of using these discrete plates is that the electric field profile is approximated by a six-segment structure, and the efficacy of non-linear reflectron operation [17] is likely degraded.

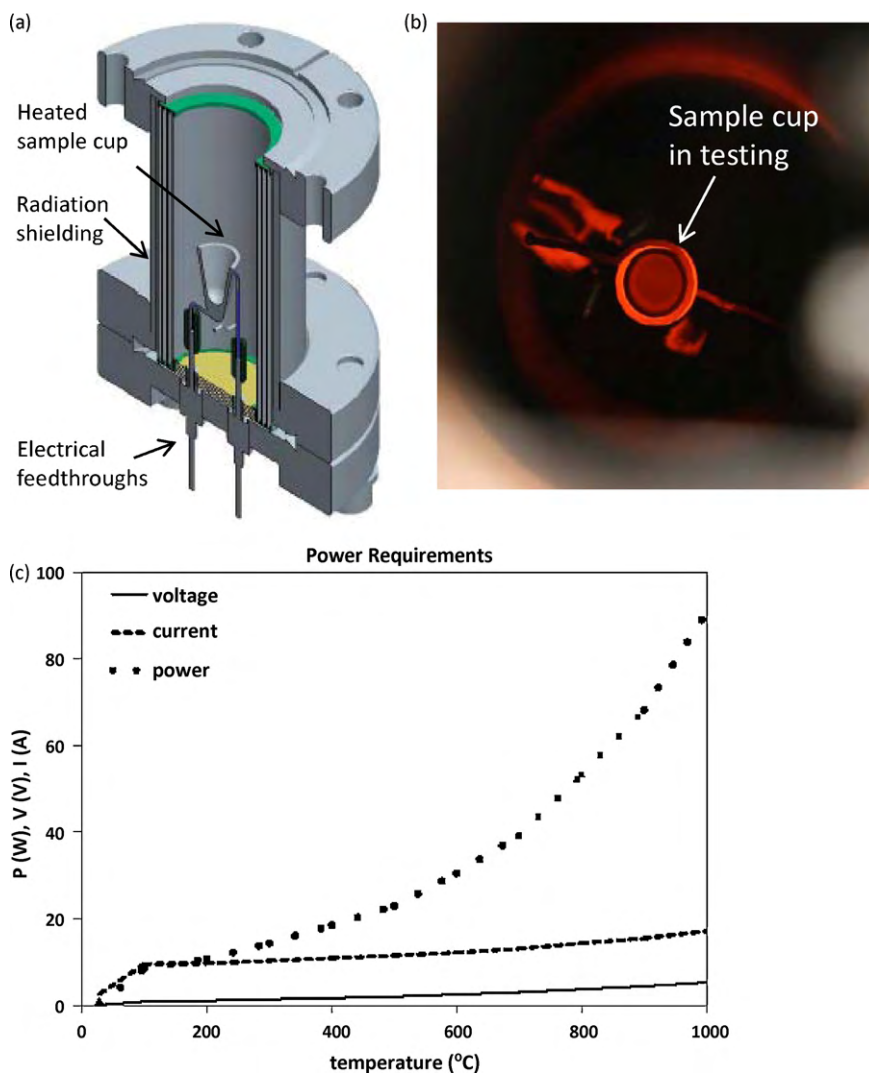


Fig. 2. Sample heater in development for solid sample pyrolysis and subsequent analysis by MS. (a) The design of the heater includes a conical coil-wound boat, coated with zirconia, layered radiation shielding, and electrical feedthroughs for operation under ultra-high vacuum. (b) Extensive testing has been conducted to measure sample temperature with applied power under relevant vacuum conditions. (c) Power, voltage, and current consumption for a typical oven run. Approximately 10 mg soil was heated to 1000 °C with a constant ramp of 20 °C/min.

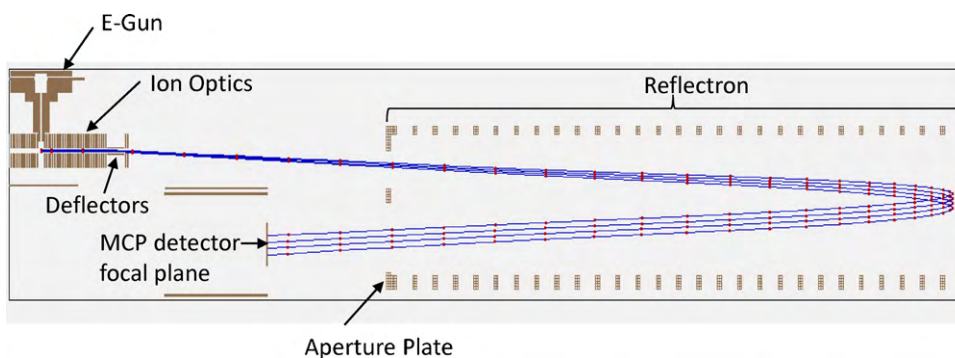


Fig. 3. SIMION model of the reflectron ToF-MS. Simulated ions are generated in the ionization region, and electric potentials are set for the ion source, the steering plates or deflectors, and the reflectron electrodes. This approach was used during instrument design to predict performance based on physical geometry and operational configuration.

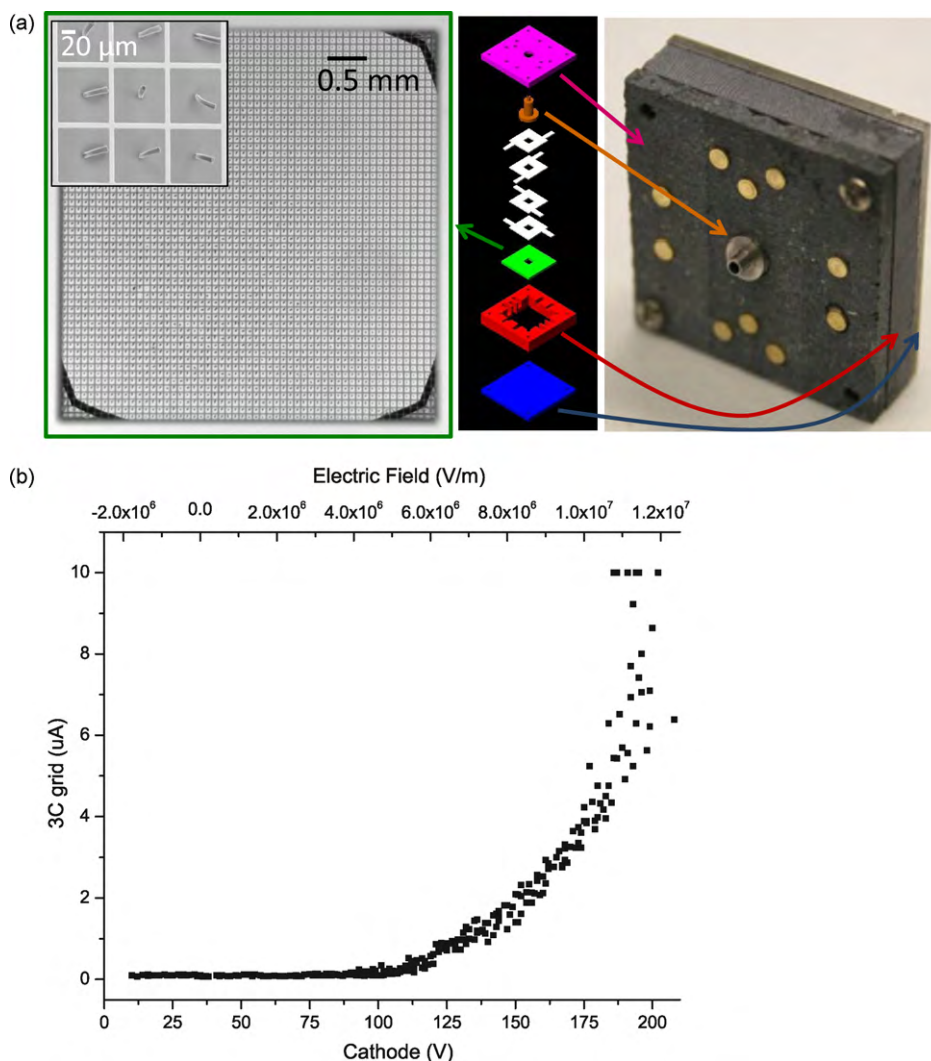


Fig. 4. (a) The electron gun is constructed from ultra-clean materials, including silicon, glass, metal, and Rescor[®] machinable ceramic. The cathode-grid component is positioned at the base of the housing, and a stack of silicon lenses is assembled at the output of the grid. The cylindrical metal aperture interfaces to the ionization region of the ion source. (b) Field emission current vs. applied grid voltage (bottom) and electric field (top). The turn-on threshold for this cathode is near 100 V (5 V/μm), and 10 μA is obtained near 175 V (11 V/μm). Fowler–Nordheim tunneling theory describes the non-linear behavior of current emission in this device.

4. Field emission electron gun

The field emission electron gun under development for VAPoR (Fig. 4) consists of a cathode-grid assembly to generate electrons that are focused using a series of discrete electrostatic lenses. The electrons then enter the ionization region through a cylindrical aperture to shield the lens packaging at the outlet of the electron gun and at the interface to the ionization region from the charged particle beam. An anode is positioned at the base of the ionization region to monitor electron beam current during operation. The cathode, grid, and electron lens elements are manufactured of silicon. For efficient ionization of gaseous species, low voltage (70–100 eV) electron emission is desirable. This corresponds to a small spacing between the cathode and extraction grid, such that the electric field (=voltage/spacing) is adequate to produce the required beam current. Pyrex[®] spacers are used to achieve the desired spacing while electrically isolating the cathode from the grid, because of its compatibility with the anodic bonding silicon assembly techniques used to fix the grid to the spacer. The lens are separated by Rescor[®] packaging. The outlet aperture is fabricated from non-magnetic stainless steel and spot welded to an electrical

lead, for control of the electric field profile throughout the stack. Electrical connections are formed by spring-loaded, gold-coated pins in contact with each of the lens tabs and the grid, and the cathode is contacted at the base with a metal plate.

The cathode consists of an array of highly redundant towers of carbon nanotubes (CNTs) that generate the electron beam using field emission. A description of the microfabrication procedure of these CNTs is described in detail elsewhere [18]. Briefly, a doped silicon wafer is etched to produce a mesa, or platform, for CNT array placement. The mesa height determines the ultimate spacing between the cathode and grid. On top of each mesa, an array of CNT catalyst islands is deposited; the location of these islands serves to template CNT growth by thermal chemical vapor deposition. Each tower measures 5 μm × 5 μm in cross-section. The tower height is determined by the catalyst thickness [19] and can vary between 15 μm and 30 μm. It is important to note that CNT height within a given device is highly uniform, however. Each tower contains approximately 1000 CNTs, and the tower array contains 54 × 54 elements spaced by 50 μm within a 3 mm × 3 mm area. This large degree of redundancy is intended to prolong the lifetime of the overall device,

even when single CNTs are degraded by ion bombardment and oxidation.

The grid is microfabricated from a silicon-on-insulator (SOI) wafer. A 10- μm thick device layer is etched into a pattern commensurate with the CNT tower array, with through-holes measuring 50 μm \times 50 μm and bar width measuring 5 μm . The thick handle layer of the SOI wafer is through-etched from the back side to form a large aperture for beam transmission to the silicon lens stack. For efficient transmission of the electron beam, the cathode towers are aligned to the perforations in the grid wafer to within 2–3 μm in the plane. The assembled cathode-grid element is then integrated with the lens elements and aperture into a Rescor[®] housing for electrical contact and ToF-MS integration.

Laboratory testing and characterization of the ToF-MS prototype is performed in a vacuum chamber with base pressure 10^{-7} Torr, equipped with high voltage (low current) electrical feedthroughs. High voltage power supplies (EMCO) provide voltages during ToF-MS operation, while a LabVIEW interface provides DC voltage control and fast voltage switching is provided by high voltage pulsers. The ion detector is a microchannel plate chevron assembly (Photonis, Inc.), and ion counts are read out by a time-of-flight board (FAST ComTec P7887), configured for a 1 ns time bin width for the experiments discussed here, and data are acquired by commercial software.

5. Preliminary pyrolysis and ToF-MS experiments and results

The two major components of VAPoR, the pyrolysis unit and the time-of-flight mass spectrometer, are the subject of parallel development and testing efforts. Each component is housed in a dedicated vacuum test facility for characterization and preliminary results are described below.

5.1. The pyrolysis unit

Pyrolysis experiments were conducted by inserting soil samples into the RD Mathis zirconia coated tungsten wire crucible, which was mounted by knife edge seal onto a stainless steel vacuum cross. This cross was equipped with a turbo-pumping station (Pfeiffer Vacuum TSU071E, TC600) to maintain ultra-high vacuum ($\sim 10^{-8}$ mbar) and a commercial residual gas analyzer (Stanford Research Systems RGA 300, 1–300 amu) to analyze the evolved gases. Approximately 10 mg of soil sample was weighed out in a quartz sleeve and placed inside the zirconia crucible. The crucible was then heated from ambient temperature to 1000 $^{\circ}\text{C}$ at a rate of 20 $^{\circ}\text{C}/\text{min}$ using a high voltage power supply (Kikusui PAN70-5A), and the voltage and current were recorded as a function of temperature. The temperature was controlled and monitored using a type C thermocouple and an Omega temperature controller. Fig. 2(c) shows a typical voltage and current profile as a function of cup temperature. Fig. 5(a) and (b) shows the inorganic and organic evolved gas results, respectively, of a lunar analog soil sample from Mauna Kea heated under the same conditions.

5.2. The time-of-flight mass spectrometer

Prior to integrating the electron gun with the ToF-MS prototype, baseline field emission measurements are performed in a diode or triode configuration, i.e., measuring current collected at the grid or placing an anode at the grid output, respectively. All elements can be voltage biased independently using high voltage DC power supplies (SRS PS350), and current is measured at the grid and anode using a dropping resistor method.

In contrast to thermionic emission using hot filaments, field emitters use only electric field to extract an electron beam from a

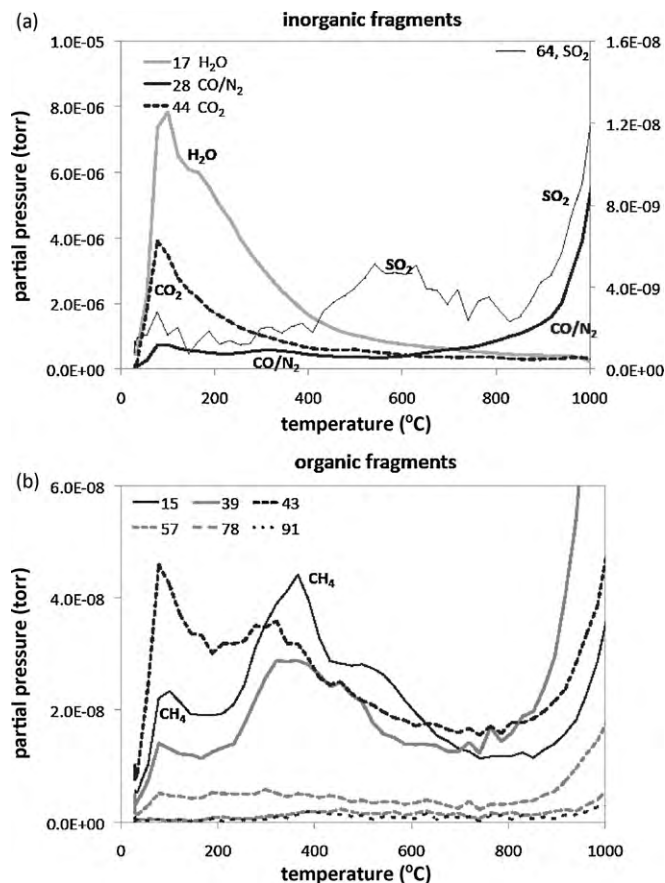


Fig. 5. (a) Selected inorganic volatiles released from the Mauna Kea soil sample as function of sample temperature. CO and N₂ cannot be separated with the RGA used and are therefore plotted together. H₂O, CO/N₂, and CO₂ are plotted on the right y-axis, SO₂ on the left y-axis. Mass 17 is used to represent H₂O, because of the high water content of the sample. Mass 18 has an $\sim 4\times$ higher partial pressure. (b) Selected alkane and aromatic hydrocarbons released from the Mauna Kea soil sample as function of sample temperature. Mass 15 corresponds to a fragment of CH₄; masses 39, 43, and 57 correspond to various alkane fragments, and masses 78 and 91 correspond to benzene, and alkylbenzene (toluene), respectively.

conductive, low work-function material. In the case of CNTs [20,21], as well as micromachined emission tips [22] and a number of other materials [23,24], a sharp conductive tip can be used to focus the local electric field lines, producing a field enhancement effect. The field enhancement effectively reduces the global electric field needed for emission and therefore the voltage for a fixed gap. This phenomenon is described by Fowler–Nordheim tunneling:

$$J = K_1 E^2 \exp\left(-\frac{K_2}{E}\right)$$

where J is the current density, K_1 is a constant, E is the global electric field, and K_2 is a constant that reflects the work function of the material and the geometrical field enhancement factor. We have determined that our CNT field emission devices are characterized by a field enhancement factor of approximately 900 [25 and references therein], which is consistent with values for similar materials that have been previously reported in the literature.

An example of the CNT field emission characteristic is shown in Fig. 4(b). As a negative voltage on the cathode is varied, the emission current is observed to modulate according to the modified exponential behavior predicted by Fowler–Nordheim theory. A current–voltage characteristic is obtained for each cathode prior to integrating with the ToF-MS for instrument testing.

We have found that the field emission properties of the CNT arrayed cathode are consistent between devices. Each device has

nominally identical tower cross-section, spacing, and outer array dimensions. Variability in the x - y grid alignment to the cathode tower array is $\pm 3 \mu\text{m}$ or less. Accounting for slight differences in cathode-grid spacing, due to variability in CNT tower height, we can calculate the global electric field needed to produce a given electron beam current density. The Fowler–Nordheim tunneling behavior is seen to be in good agreement between the devices, suggesting that the nano- and microfabrication techniques employed in this device development enable manufacturability of nanostructured field emitters.

After baseline testing to characterize the field emission from the cathode, a cathode-grid component of the type shown in Fig. 4 was mounted into the lens assembly housing for integration with the time-of-flight mass spectrometer prototype. Once the cathode-grid component and electron beam lenses are mounted into the modular electron gun housing, the assembly is inverted and installed onto the ion lens assembly. The aperture is press-fit into a through-hole in the ion lens housing, and this serves to align the electron beam with respect to the acceleration electrodes that are voltage-modulated in ion extraction mode. The aperture's length does not protrude into the ionization region, in order to prevent perturbations on the ion population during formation and extraction. In the following experiments, the ionization current supplied by the electron gun is approximately $0.05 \mu\text{A}$ at the anode. The beam current supplied by the cathode is nearly 100 times greater than this, but the geometrical constraints imposed by the aspect ratio of the aperture reduce the transmitted current significantly.

There are eight ion lenses that control the electric field gradients experienced by the ions that result from electron impact processes. Two are positioned on either side of the electron beam along the ion trajectory to define the pulsed extraction potential. For the measurements discussed here, the ion extraction voltage is pulsed by 200 V to accelerate the ions toward the detector. The remaining four ion lenses are seen by the ions as they exit the ion source into the analyzer and can be used for focusing or acceleration. In addition, there is a set of steering plates at the output of the ion source to allow deflections of the ion beam for signal optimization at the detector.

It should be noted that the electron beam itself is not pulsed on and off during the ionization and extraction processes, respectively. This has the effect of contributing “untimed” ions to the packet; that is, after the majority of the ions have been accelerated from the ionization region, a trickle of ions is generated and continuously extracted toward the analyzer. The severity of the effect is mitigated by the deflection of the electron beam toward the back plane of the ionization region during pulsed extraction, thereby limiting the number of ions that are ultimately transmitted to the detector. However, the effect is expected to be detrimental to the signal to noise ratio of the instrument, and approaches to beam pulsing are under consideration for future work. One straightforward method is the incorporation of deflection plates at the output of the electron gun. A more elegant approach would be to pulse the emission voltage directly, and we intend to investigate this possibility in future testing.

The sample ions exit the ion lens assembly with a well defined kinetic energy and travel through a field-free region into the analyzer. In linear mode, the analyzer acts simply as a field-free flight tube, allowing the ion packets to separate according to mass. Throughout the following discussion, we do not treat the sensitivity of the instrument, as this is the subject of continuing work. As a result, the detector counts shown for each spectrum do not represent constant signal accumulation duration. We emphasize, therefore, that detector counts cannot be compared quantitatively between spectra.

With the chamber pressure at 4×10^{-7} Torr, we obtained a baseline mass spectrum in linear mode using the chamber background

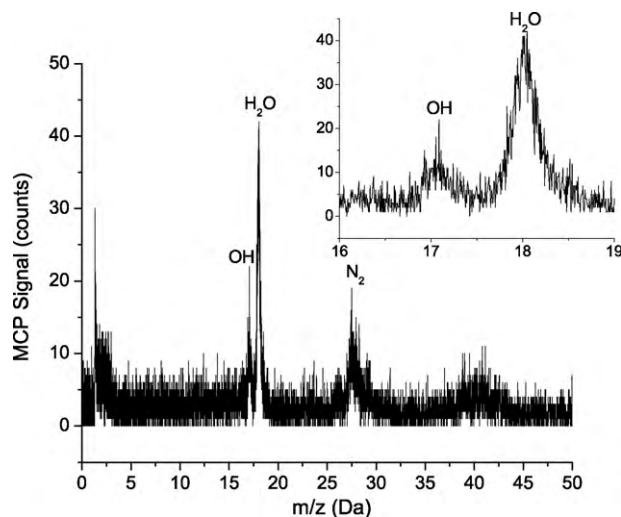


Fig. 6. Detector counts vs. mass-to-charge ratio for linear mode of the prototype ToF-MS. This spectrum was acquired using a carbon nanotube field emission cathode with ionization current of $0.05 \mu\text{A}$. Residual chamber gases were used for these measurements. (Inset) Separation of hydroxyl and water peaks is evident, though it should be noted that the prototype is not optimized for linear mode.

gases as the sample, as shown in Fig. 6. It is important to note that the mass resolution presented here for linear detection is not optimized because the ion lens voltages were approximately configured for reflectron mode. As a result, the linear mode mass spectra do not represent the best case for ion packet focusing.

A residual gas analyzer (SRS RGA300) is mounted onto the chamber for the purpose of a control measurement, allowing corroboration of mass calibration parameters with experimental time-of-flight peak positions. Using the RGA, the dominant background species in the vacuum chamber were determined to be nitrogen and water, as expected. These peaks are easily identified in our mass spectrum at masses 18 and 28 Da.¹ The OH peak is also seen at 17 Da, and it is clearly resolved from the H₂O peak, even in the case of diminished ion focusing in linear mode.

We have also characterized reflected mode operation of the ToF-MS prototype. Instead of using the analyzer region as a field-free flight volume, the reflectron lenses are voltage biased to produce a decelerating field profile. The direction of the ion packets is reversed, and the ions are registered at a second detector position beneath the ion source. To accomplish this ion mirror effect, the five-segment reflectron was biased with a curved field profile approximating one quadrant of a circle to achieve the increased path length and enhanced focus described above.

Here, a curved-field reflectron configuration is used in order to explore the resolution capabilities of the instrument. It should be recognized, however, that using a non-linear reflectron profile of this type will reduce ion transmission through the analyzer. Some sensitivity may be regained by using a linear reflectron, and this “intermediate” regime will be investigated in future instrument characterization efforts.

An early mass spectrum acquired in reflectron mode is shown in Fig. 7. The inset reveals that the peak separation between the hydroxyl and water peaks is improved by 25% compared to linear mode, owing to the increased flight path with the use of the reflectron. Furthermore, the peak width is sharpened by a factor of 5,

¹ We acknowledge that the 28 Da peak represents a mixture of N₂ and carbon monoxide, since the lower mass resolution shown here ($\sim 200\text{m}/\Delta m$) is insufficient to resolve the slight mass difference between the two species which would require a mass resolution $\sim 2500\text{m}/\Delta m$. Owing to the low partial pressure of CO₂, however, as determined by the RGA, we infer that the dominant constituent here is N₂.

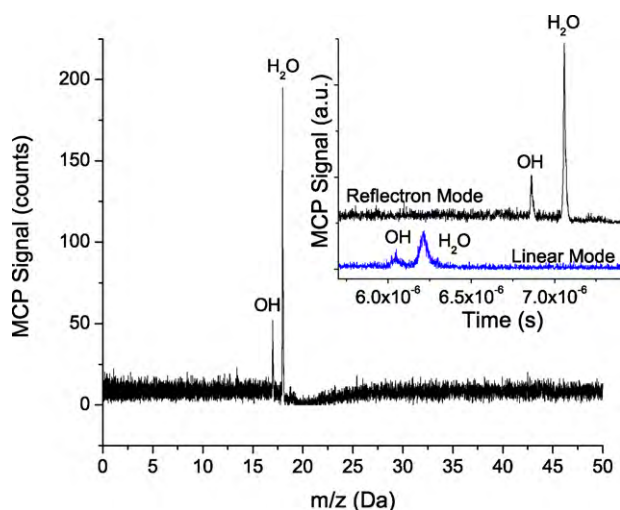


Fig. 7. Detector counts vs. mass-to-charge ratio for reflectron mode of the prototype ToF-MS. The hydroxyl and water peaks are reproduced here, but the nitrogen has low partial pressure, relative to the dominant water signal. This is attributed to a recent venting of the chamber and high pumping efficiency of N_2 . (Inset) Detector signal vs. time-of-flight is shown for reflectron (upper) and linear (lower) modes. Note that these data are offset in Y for clarity. Therefore, the y-axis is expressed in arbitrary units (a.u.). Improvements in peak separation and peak width are noticeable with use of the reflectron.

which indicates the improved ion focus obtained at the plane of the detector. This is due to design considerations and is expected from SIMION simulations.

The dominant peaks of OH and H_2O are again observed in the reflected spectrum, as in the linear spectrum discussed above. Nitrogen is absent, and although we have not identified the exact cause, it may be potentially due to a higher relative partial pressure of water vapor from a prolonged exposure of the chamber walls to ambient air prior to the measurements, which is due to higher efficiency of turbo molecular pump for N_2 .

In an effort to maintain N_2 pressure in subsequent tests, we introduced high-purity N_2 gas into the chamber through a metered valve. We can therefore make a direct comparison between the linear- and reflectron-mode mass spectra, as shown in Fig. 8. Agreement between peak positions is seen to be very good.

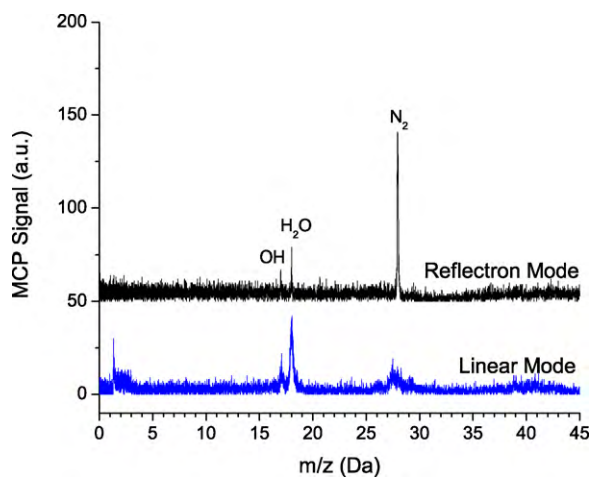


Fig. 8. Detector counts vs. mass-to-charge ratio the prototype ToF-MS. Linear mode (lower) and reflectron mode (upper) show reproducible peak locations for OH, H_2O , and N_2 , the major constituents in the chamber. Note that these data are offset in Y for clarity. Therefore, the y-axis is expressed in arbitrary units (a.u.). Vast improvements to mass resolution are evident in the sharper peaks produced by reflectron mode. This is expected from longer path length and improved ion focus at the plane of the reflected detector.

As expected from SIMION simulations, the mass resolution is improved significantly with the use of the reflectron. A direct comparison of the temporal separation between mass 17 and mass 18 is shown in the inset of Fig. 8. Since the instrument mass resolution, described in the mass or time domain, is given by

$$\text{Resolution} = \frac{m}{\Delta m} = \frac{t}{2\Delta t}$$

we can determine the linear mass resolution to be a value of approximately 19. The reflected mass resolution, in contrast, is improved by over an order of magnitude at approximately 270.

As discussed briefly above, the sensitivity of the ToF-MS prototype is currently not adequate to meet our performance goals. This is largely due to the attenuation of electron beam current transmission into the ionization region. One culprit of reduced electron transmission is the cylindrical aperture that forms the interface between the electron gun and the ion lens assembly.

The length of the aperture is driven by the combined thickness of the electron gun lid and the ion lens assembly entry point, which is a through-hole in a Macor insulating plate. This length (approximately 5 mm) is therefore comparable to the electron beam path through the lens assembly (3 mm), rendering the lensing system ineffective. In other words, higher voltages are required in the presence of the long aperture, than would be required in its absence, to accelerate and focus the electrons into the ionization region, by virtue of the distance between the lens stack and the mid-point in the ion lens structure. Because the present design emphasizes modularity, the transmission efficiency and final kinetic energy of the electron beam during ionization are not optimized. Here, the transmission is only a few percent of the electron beam current, severely limiting the sensitivity of the mass spectrometer. The kinetic energy, in turn, is approximately 500 eV, at least 5 times higher than the desired electron beam energy for most efficient gas-phase ionization.

Improvements to this design are presently under consideration. In future development efforts, the aperture will be eliminated and the ion lens assembly and electron gun assembly will be closely integrated. SIMION simulations of this structure indicate that significant improvements can be made to the electron beam transmission efficiency, as well as the terminal kinetic energy of the electrons.

6. Conclusions

We have demonstrated the design, simulation, fabrication, and testing of two components of VAPoR, a pyrolysis oven and a miniature ToF-MS for use in mass- and power-constrained planetary science missions to study the mineralogy and geochemistry of planetary surfaces.

The VAPoR prototype, in both laboratory and field testing, has demonstrated characterization of analog samples relevant to planetary science, including volcanic rock samples from the Mauna Kea volcano in Hawaii.

In parallel prototype development, we have employed micro- and nanofabrication techniques to develop a miniaturized mass spectrometer that exhibits a mass resolution of 270 at mass 18 (water). With further integration of our field emission cathode with the ion source and time-of-flight analyzer, we anticipate sensitivity improvements to achieve higher performance.

Acknowledgements

The authors would like to acknowledge support from the NASA Astrobiology Science and Technology Instrument Development Program (07-ASTID07-0020), the GSFC Internal Research and

Development Program, and the Field Science Analog Testing Program.

References

- [1] I.L. ten Kate, E.H. Cardiff, J.P. Dworkin, S.H. Feng, V. Holmes, C. Malespin, J. Stern, T.D. Swindle, D.P. Glavin, VAPoR—Volatile Analysis by Pyrolysis of Regolith—an instrument for in situ detection of water, noble gases, and organics on the Moon, *Planetary and Space Science* (2010), doi:10.1016/j.pss.2010.03.006.
- [2] J.H. Hoffman, R.C. Chaney, H. Hammack, *Journal of the American Society for Mass Spectrometry* 19 (October (10)) (2008) 1377–1383.
- [3] P.R. Mahaffy, Exploration of the habitability of Mars: development of analytical protocols for measurement of organic carbon on the 2009 Mars Science Laboratory, *Space Science Reviews* 135 (2008) 255–268.
- [4] A.R. Vasavada, the MSL Science Team, NASA's 2009 Mars Science Laboratory: an update [abstract 1940], in: 37th Lunar and Planetary Science Conference Abstracts, Lunar and Planetary Institute, 2006.
- [5] J.H. Waite, S. Lewis, W.T. Kasprzak, V.G. Anicich, B.P. Block, T.E. Cravens, G.G. Fletcher, W.H. Ip, J.G. Luhmann, R.L. McNutt, H.B. Niemann, J.K. Parejko, J.E. Richards, R.L. Thorpe, R.M. Walter, R.V. Yelle, The Cassini ion and neutral mass spectrometer (INMS) investigation, *Space Science Reviews* 114 (2002) 113–231.
- [6] H. Niemann, S. Atreya, S. Bauer, K. Biemann, B. Block, G. Carignan, T. Donahue, R. Frost, D. Gautier, J. Haberman, D. Harpold, D. Hunten, G. Israel, J. Lunine, K. Mauersberger, T. Owen, F. Raulin, J. Richards, S. Way, The gas chromatograph mass spectrometer for the Huygens probe, *Space Science Reviews* 104 (2002) 553–591.
- [7] H. Balsiger, K. Altwegg, P. Bochsler, P. Eberhardt, J. Fischer, S. Graf, A. Jackel, E. Kopp, U. Langer, M. Mildner, J. Muller, T. Riesen, M. Rubin, S. Scherer, P. Wurcz, S. Wuthrich, E. Arijis, S. Delanoye, J. De Keyser, E. Neefs, D. Nevejans, H. Reme, C. Aoustin, C. Mazelle, J.L. Medale, J.A. Sauvaud, J.J. Berthelier, J.L. Bertaux, L. Duvet, J.M. Illiano, S.A. Fuselier, A.G. Ghielmetti, T. Magoncelli, E.G. Shelley, A. Korth, K. Heerlein, H. Lauche, S. Livi, A. Loose, U. Mall, B. Wilken, F. Gliem, B. Fiethe, T.I. Gombosi, B. Block, G.R. Carignan, L.A. Fisk, J.H. Waite, D.T. Young, H. Wollnik, Rosina—Rosetta orbiter spectrometer for ion and neutral analysis, *Space Science Reviews* 128 (1–4) (2007) 745–801.
- [8] D.M. Anderson, K. Biemann, G.P. Shulman, P. Toulmin, H.C. Urey, T. Owen, L.E. Orgel, J. Oro, Mass-spectrometric analysis of organic compounds, water and volatile constituents in atmosphere and surface of Mars—Viking Mars lander, *Icarus* 16 (1) (1972) 111–138.
- [9] R.T. Chamberlin, The gases in rocks, in: *Contributions to Cosmogony and the Fundamental Problems of Geology*, Carnegie Institution of Washington Publication, 1908, p. 106.
- [10] E.S. Shepherd, The gases in rocks and some related problems, *American Journal of Science* 111 (1935) 311–351.
- [11] C.G. Barker, Mass spectrometric analysis of the gas evolved from some heated natural minerals, *Nature* 205 (1965) 1001–1002.
- [12] H.L.C. Meuzelaar, W. Windig, A.M. Harper, S.M. Huff, W.M. McClennen, J.M. Richards, Pyrolysis mass spectrometry of complex organic materials, *Science* 226 (1984) 268–274.
- [13] K. Biemann, J. Oro, P. Toulmin III, L.E. Orgel, A.O. Nier, D.M. Anderson, P.G. Simmonds, D. Flory, A.V. Diaz, D.R. Rushneck, J.E. Biller, A.L. Lafleur, The search for organic substances and inorganic volatile compounds in the surface of Mars, *Journal of Geophysical Research* 82 (1977) 4641–4658.
- [14] W.V. Boynton, S.H. Bailey, D.K. Hamara, M.S. Williams, R.C. Bode, M.R. Fitzgibbon, W.J. Ko, M.G. Ward, K.R. Sridhar, J.A. Blanchard, R.D. Lorenz, R.D. May, D.A. Paige, A.V. Pathare, D.A. Kring, L.A. Leshin, D.W. Ming, A.P. Zent, D.C. Golden, K.E. Kerry, H.V. Lauer, R.C. Quinn, Thermal and evolved gas analyzer: part of the Mars volatile and climate surveyor integrated payload, *Journal of Geophysical Research—Planets* 106 (E8) (2001) 17683–17698.
- [15] F. Goesmann, H. Rosenbauer, R. Roll, C. Szopa, F. Raulin, R. Sternberg, G. Israel, U. Meierhenrich, W. Thiemann, G. Munoz-Caro, COSAC, the cometary sampling and composition experiment on Philae, *Space Science Reviews* 128 (1–4) (2007) 257–280.
- [16] I.P. Wright, S.J. Barber, G.H. Morgan, A.D. Morse, S. Sheridan, D.J. Andrews, J. Maynard, D. Yau, S.T. Evans, M.R. Leese, J.C. Zarnecki, B.J. Kent, N.R. Waltham, M.S. Whalley, S. Heys, D.L. Drummond, R.L. Edeson, E.C. Sawyer, R.F. Turner, C.T. Pillinger, Ptolemy—an instrument to measure stable isotopic ratios of key volatiles on a cometary nucleus, *Space Science Reviews* 128 (1–4) (2007) 363–381.
- [17] T.J. Cornish, R.J. Cotter, A curved-field reflectron for improved energy focusing of product ions in time-of-flight mass spectrometry, *Rapid Communications in Mass Spectrometry* 7 (1993) 1037.
- [18] S.A. Getty, M. Li, L. Hess, N. Costen, T.T. King, P.A. Roman, W.B. Brinckerhoff, P.R. Mahaffy, Integration of a carbon nanotube field emission electron gun for a miniaturized time-of-flight mass spectrometer, in: *Proceedings of the SPIE*, vol. 7318, 2009, p. 731816.
- [19] S.A. Getty, R.A. Bis, S. Snyder, E. Gehrels, K. Ramirez, T.T. King, P.A. Roman, P.R. Mahaffy, Effect of nitrogen gas on the lifetime of carbon nanotube field emitters for electron-impact ionization mass spectrometry, in: *Proceedings of the SPIE*, vol. 6959, 2008, p. 695907.
- [20] W.A. de Heer, A. Chatelain, D. Ugarte, A carbon nanotube field-emission electron source, *Science* 270 (1995) 1179.
- [21] A.G. Rinzler, J.H. Hafner, P. Nikolaev, L. Lou, S.G. Kim, D. Tomanek, P. Nordlander, D.T. Colbert, R.E. Smalley, Unraveling nanotubes: field emission from an atomic wire, *Science* 269 (1995) 1550.
- [22] C.A. Spindt, A thin-film field-emission cathode, *Journal of Applied Physics* 39 (7) (1968) 3504–3505.
- [23] A.A. Talin, B. Chalamala, B.F. Coll, J.E. Jaskie, R. Petersen, L. Dworsky, Development of field emission flat panel displays at Motorola, *Materials Research Society Symposium Proceedings* 509 (1998) 21–23.
- [24] A.R. Krauss, O. Auciello, M.Q. Ding, D.M. Gruen, Y. Huang, V.V. Zhirnov, E.I. Givargizov, A. Breskin, R. Chechen, E. Shefer, V. Konov, S. Pimenov, A. Karabutov, A. Rakhimov, N. Suetin, Electron field emission for ultrananocrystalline diamond films, *Journal of Applied Physics* 88 (11) (2000).
- [25] S.A. Getty, T.T. King, R.A. Bis, H.H. Jones, F. Herrero, B.A. Lynch, P. Roman, P. Mahaffy, Performance of a carbon nanotube field emission electron gun, in: *Proceedings of SPIE*, vol. 6556, 2007, p. 18.